Received: 15 February 2023 | Revised: 3 July 2023 | Accepted: 6 August 2023

DOI: 10.1002/joc.8220

RESEARCH ARTICLE

International Journal of Climatology RMetS

Asymmetric influence of the Pacific meridional mode on tropical cyclone formation over the western North Pacific

Jinjie Song[1,2] | Philip J. Klotzbach[3] | Yi-Fan Wang[1] | Yihong Duan[2]

[1]Nanjing Joint Institute for Atmospheric Sciences, Chinese Academy of Meteorological Sciences, Nanjing, China

[2]State Key Laboratory of Severe Weather, Chinese Academy of Meteorological Sciences, Beijing, China

[3]Department of Atmospheric Science, Colorado State University, Fort Collins, Colorado, USA

Correspondence
Yihong Duan, State Key Laboratory of Severe Weather, Chinese Academy of Meteorological Sciences,
46 Zhongguancun South Avenue,
Beijing 100081, China.
Email: duanyh@cma.gov.cn

Funding information
G. Unger Vetlesen Foundation; National Natural Science Foundation of China, Grant/Award Numbers: 42192554, 61827901, 42175007, 41905001, 42192552

Abstract

This study investigates the asymmetric response of western North Pacific (WNP) tropical cyclone (TC) formation during August–November to the Pacific meridional mode (PMM) from 1961 to 2021. Basinwide WNP TC frequency significantly increases (slightly decreases) during positive (negative) PMM years, implying a nonlinear PMM–TC frequency relationship. Only small spatial changes in TC formation occur during negative PMM years, while there is nearly a basinwide enhancement of TC formation during positive PMM years, particularly over the region of 5°–30°N and 135°–155°E. This region is characterized by significantly enhanced low-level vorticity, mid-level updrafts and upper-level divergence during positive PMM years, all favouring TC development. By contrast, environmental anomalies are of a smaller magnitude and mostly insignificant over the WNP during negative PMM years. These distinct environmental changes during different PMM phases can be explained by differences in PMM strength. Positive PMM events are of a greater strength and are associated with a stronger wind–evaporation–sea surface temperature feedback than negative PMM events, leading to a notable anomalous large-scale low-level cyclonic circulation over the WNP in positive PMM events.

KEYWORDS

Pacific meridional mode, tropical cyclone, western North Pacific

1 | INTRODUCTION

Tropical cyclones (TCs) are one of the most destructive and deadliest natural disasters around the world, posing a severe threat to life and property in coastal regions. The western North Pacific (WNP) is the most TC-active basin worldwide, where approximately one-third of global TCs develop on an annually averaged basis (Lee et al., 2012). Given the heightened awareness of climate change, increasing attention has been paid to the temporal variability of TC activity as modulated by various climate modes (Walsh et al., 2016). It is by now well known that El Niño–Southern Oscillation (ENSO) is a major factor modulating WNP TC activity on interannual timescales. ENSO has been shown to significantly influence interannual changes in frequency, intensity, formation location and lifespan of WNP TCs (Emanuel, 2018).

Recently, the Pacific meridional mode (PMM) has been shown to be another important factor modulating WNP TC activity. Zhang et al. (2016) reported a significant interannual correlation between the PMM and WNP TC frequency. The regressions of TC track density onto the PMM highlight a basinwide enhancement (suppression) of TC activity during the positive (negative) PMM phase, which has been attributed to PMM-induced changes in environmental vertical wind shear (VWS) and the low-level large-scale circulation over the WNP (Zhang et al., 2016). Gao et al. (2018) and Gao et al.

(2020) found a significant positive relationship between the PMM and the frequency of intense TCs over the WNP and landfalling TCs in China. During positive phases of the PMM, the anomalous low-level cyclonic circulation not only increases TC formation over the main development region but also favours TCs moving westward/northwestward and making landfall in China (Gao et al., 2018; Gao et al., 2020).

Given the strong relationship between PMM and ENSO (Stuecker, 2018), other studies have further examined the PMM–TC relationship independent of ENSO. Hong et al. (2018) showed that ENSO and the PMM dominated south–north and east–west migrations of mean TC formation position over the WNP, respectively. Zhang et al. (2020) attributed the significant positive relationship between the PMM and WNP TC frequency to the frequent concurrence of PMM and ENSO. They argued that the PMM itself had a limited impact on WNP TC formation, since it only weakly affected the tropical circulation, the subtropical high and the monsoon trough over the WNP.

On the other hand, Wu et al. (2020) found that after excluding ENSO events, the PMM had a basin-scale impact on the WNP circulation, subsequently inducing a near-uniform change in WNP TC formation. These disparate results may arise from different criteria used to identify PMM events, which can be mainly attributed to the different PMM indices used in these two studies. The PMM index was calculated as the area-averaged sea surface temperature (SST) anomaly (SSTA) over the subtropical eastern Pacific (10°–25°N, 160°–120°W) in Zhang et al. (2020), while it was derived from a singular value decomposition based on SSTAs and surface wind anomalies over the region of 21°S–32°N and 175°E–95°W in Wu et al. (2020).

All of the aforementioned publications studying the modulation of WNP TC activity by the PMM have done so by correlating and regressing variables onto the PMM index or computing differences between positive and negative PMM phases (Fu et al., 2023; Gao et al., 2018, 2020; Hong et al., 2018; Wu et al., 2020; Zhang et al., 2016, 2020). These studies mostly assumed that changes in WNP TC activity for positive PMM events would mirror those for negative PMM events. By comparison, some studies have noticed an asymmetric response of WNP TC activity to ENSO. When focusing on the decay period of ENSO from May to July, Li et al. (2018) found an asymmetry in the response of the longitudinal location of TC formation to eastern Pacific (EP) ENSO events. Average TC formation location migrated more westward in response to more intense EP El Niño, while it was nearly unrelated to the intensity of EP La Niña. This was mainly attributed to the intensity asymmetry of large-scale environmental variables between EP El Niño and EP La Niña. Li et al. (2018) also showed that although the intensity of central Pacific (CP) El Niño and La Niña was comparable, CP El Niño tended to more strongly modulate WNP TC activity than CP La Niña. In addition, Li et al. (2023) reported that during negative decades of the North Atlantic tripole SSTA pattern, significantly fewer northward moving TCs over the WNP were observed in El Niño following years, while northward moving TC frequency remained almost unchanged in La Niña following years.

Using the Community Earth System Model, Thomas and Vimont (2016) found an asymmetry in SST and wind anomalies during positive and negative PMM phases. They showed that during September–November, significant anomalous westerlies occurred west of 150°E during a positive PMM, while there were almost no significant wind anomalies over the same region during a negative PMM. Fan et al. (2021) also noted that a positive PMM event enhanced El Niño more strongly than a negative PMM event enhanced La Niña, implying an asymmetric modulation of ENSO evolution by the PMM. These findings were linked to the simulated results that positive PMM events generally grew stronger than negative PMM events in the subtropics. Positive (negative) PMM events evoked stronger (weaker) changes in subtropical SST, due to a larger (smaller) transient growth rate of latent heat flux via the wind–evaporation–SST (WES) feedback (Chang et al., 1997; Xie & Philander, 1994). However, it is unclear whether there is an asymmetric response of WNP TC activity to the PMM on interannual timescales. Several studies have focused on boreal summers with a positive PMM phase and an ENSO neutral state: 2016 (Zhan et al., 2017) and 2018 (Basconcillo et al., 2021; Takaya, 2019). Relative to the long-term climatology, the WNP was much more TC-active in these positive PMM boreal summers, with a significantly higher TC frequency. By contrast, few studies have investigated characteristics of WNP TC seasons during negative PMM phases.

The primary objectives of this study are to analyse and compare the anomalous features of WNP TC formation during different PMM phases. The remainder of this paper is arranged as follows. Section 2 describes the data and methodology. Sections 3 and 4 discuss the responses of WNP TC formation and large-scale environmental conditions, respectively, to different PMM phases. Section 5 concludes the manuscript.

2 | DATA AND METHODOLOGY

This study uses 6-hourly TC best track data from the International Best Track Archive for Climate Stewardship (IBTrACS) v04r00 (Knapp et al., 2010) between 1961 and

2021. As suggested by Song and Klotzbach (2018), in order to reduce the uncertainty among data sources and enhance the robustness of the results, we only consider TCs simultaneously recorded by four warning agencies over the WNP, that is, the Joint Typhoon Warning Center, the Japan Meteorological Agency, the China Meteorological Administration and the Hong Kong Observatory. Intensity-based methods are often used to define TC formation. For instance, TC formation is defined when the TC maximum sustained wind first exceeds a threshold, such as 34 kt (e.g., Yokoi et al., 2013) or 40 kt (e.g., Daloz & Camargo, 2018). The reliability of this TC formation definition relies on the quality of the estimated absolute TC intensity, which has significant uncertainty in the pre-satellite era. To overcome this shortcoming, TC formation in this study is identified as the first record that is simultaneously listed by all four agencies. This identification can minimize possible influences of the temporal evolution of observational technologies for weak TCs (e.g., tropical depressions), as noted in Klotzbach and Landsea (2015), because stronger TCs are more likely to be tracked by multiple agencies simultaneously. The TC formation density is obtained by counting TC formation numbers over a $5^\circ \times 5^\circ$ grid and is subsequently spatially smoothed through the method proposed by Kim et al. (2011).

The WNP TC-active season is usually defined as June–November, during which ~85% of the annual total number of WNP TCs form (Song & Klotzbach, 2019). Recently, Fu et al. (2023) found that there was a season-dependent modulation of PMM on WNP TC formation, with a significant positive correlation in January–April and August–December but an insignificant relationship in May–July. Therefore, we focus on the 4-month period of August–November (ASON), which includes ~63% of the annual total number of TCs and ~74% of the TCs forming during June–November.

ASON-averaged thermodynamic and dynamic factors influencing TC formation including maximum potential intensity (MPI), 600-hPa relative humidity, 850-hPa relative vorticity, 500-hPa vertical velocity, 200-hPa divergence and lower-level (850 hPa) relative vorticity, upper-level (200 hPa) divergence and 850–200-hPa VWS are derived from two monthly datasets. One is the Hadley Centre Sea Ice and Sea Surface Temperature dataset (HadISST; Rayner et al., 2003), providing SSTs on a $1^\circ \times 1^\circ$ grid. The other is the fifth generation European Centre for Medium-Range Weather Forecasts reanalysis of the global climate (ERA5; Hersbach et al., 2020), providing atmospheric variables at a $0.25^\circ \times 0.25^\circ$ resolution. ASON-averaged PMM, Niño3 and Niño4 indices are obtained from their respective monthly SST timeseries provided by the Physical Sciences Laboratory of the National Oceanic and Atmospheric Administration. The SST-based PMM index is used in this study, given that the SST index for the PMM is more representative of the coupled mode than the wind-based PMM index (Chiang & Vimont, 2004). Our results are not significantly changed, when replacing the PMM SST index by the PMM wind index (figures not shown).

TABLE 1 List of positive (the five highest) and negative (the five lowest) PMM years during ASON from 1961 to 2021, as well as the corresponding number of WNP TCs

Positive PMM		Negative PMM	
Year	N_{TC}	**Year**	N_{TC}
1966	26	1962	20
1968	21	1980	13
1990	18	2000	15
1992	23	2008	13
2016	21	2012	14
Mean	21.8	Mean	15.0
Anomaly	5.0 ($p < 0.01$)	Anomaly	−1.8 ($p = 0.31$)

Note: Anomalies and their significance levels are calculated relative to the 1961–2021 climatology.

Given that the PMM is not fully independent of ENSO (Stuecker, 2018), we first remove El Niño and La Niña events when the magnitude of the ASON-averaged Niño3 or Niño4 SSTA exceeds 0.5°C, which excludes both EP and CP ENSO events. For the remaining 19 years, we then select the highest 5 PMM (positive PMM) years and the lowest 5 PMM (negative PMM) years based on the ASON-averaged PMM index (Table 1), accounting for approximately one-half of ENSO neutral years. Other publications (e.g., Zhan et al., 2011) have also used 5-year samples to study the influence of climate modes on changes in WNP TC activity.

The significance levels (p) of correlation coefficients (r) and the differences in means between two samples are both estimated using a two-tailed Student's t test. The significances of the regression equations and coefficients are given by an F test. In evaluating statistical significance, the effective sample size proposed by Trenberth (1984) is applied to minimize the influence of autocorrelation.

3 | ASYMMETRIC RESPONSE OF WNP TC FORMATION TO THE PMM

Figure 1a highlights a significant positive relationship between WNP TC frequency during ASON and the simultaneous PMM index from 1961 to 2021 ($r = 0.49$, $p < 0.01$). Consistent with Fu et al. (2023), during June

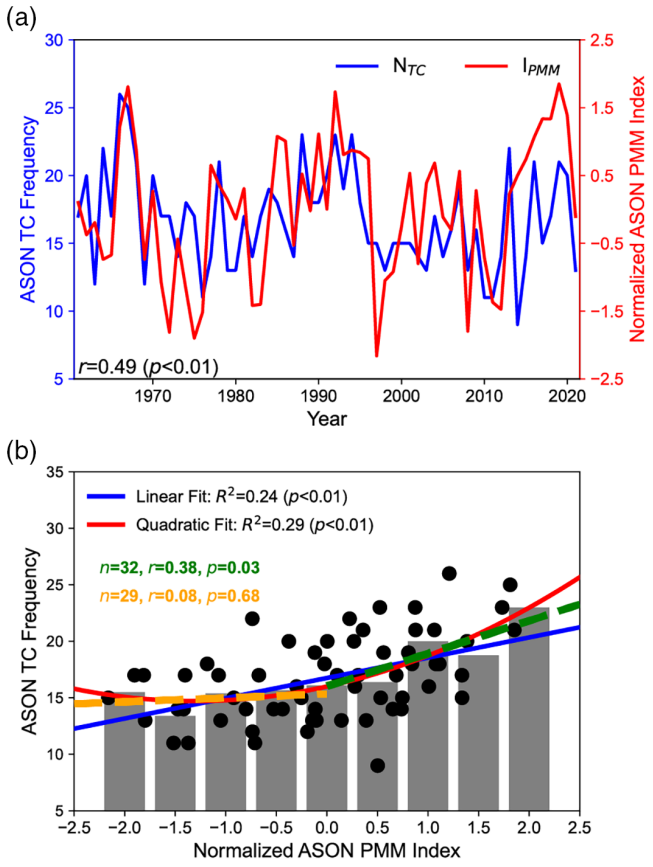

FIGURE 1 (a) Annual variations of WNP TC frequency and the normalized PMM index during ASON from 1961 to 2021. The correlation coefficient and significance level are shown in the panel. (b) Relationship between WNP TC frequency and the normalized PMM index during ASON from 1961 to 2021. The grey bar denotes the mean TC frequency for a specific PMM index. The blue and red lines refer to the best fit linear and quadratic curves, respectively, while their explained variances and significance levels are provided in the panel. Green and orange dashed lines denote the best fit linear lines for 32 positive PMM years and 29 negative PMM years, respectively. The corresponding correlation coefficients and significance levels are shown in the panel [Colour figure can be viewed at wileyonlinelibrary.com]

and July, we find a weak correlation between TC frequency and the PMM index ($r = -0.01$, $p = 0.94$). Given that TC frequency during ASON (16.8) is nearly three times that during June and July (5.8) climatologically, the significant PMM–TC frequency relationship during June–November as found in previous publications (e.g., Wu et al., 2020; Zhang et al., 2016) is dominated by the significant relationship during ASON. Liu et al. (2019) reported that TC frequency over the southeastern subdomain of the WNP showed a strong (weak) correlation with the PMM on decadal (interannual) timescales. However, after applying a 9-year Lanczos filter, as used in Liu et al. (2019), we find significant relationships between the PMM and TC frequency over the entire WNP on both decadal and interannual timescales, with correlation coefficients of 0.60 ($p < 0.01$) and 0.39 ($p < 0.01$), respectively. The discrepancy between our results and those of Liu et al. (2019) may be due to the different TC formation regions considered.

Figure 1b shows that although a quadratic function between TC frequency and the PMM explains just slightly more variance than a linear function, its quadratic coefficient is statistically significant at the 0.05 level. This means that a nonlinear PMM–TC frequency relationship is more reasonable than a linear one. When the PMM index is larger than 0.5 standard deviations, the mean TC frequency generally increases with increasing PMM index. By comparison, the mean TC frequency remains almost unchanged when the PMM index is smaller than 0.5 standard deviations. In addition, the correlation coefficient between the PMM and TC frequency is 0.38 ($p = 0.03$) for the 32 years with a positive PMM, while it is 0.08 ($p = 0.68$) for the 29 years with a negative PMM (Figure 1b). These results imply that a stronger positive PMM event is often linked to more TCs forming over the WNP, while the strength of a negative PMM event has only a small impact on WNP TC frequency.

After removing the impact of ENSO, there is also an asymmetric response of WNP TC frequency to the PMM (Table 1). There are, on average, 21.8 TCs forming over the WNP during positive PMM years, which is 5.0 TCs greater than the 1961–2021 climatology ($p < 0.01$) and 4.7 TCs greater than the mean during PMM neutral years ($p = 0.02$). By contrast, the average TC frequency during negative PMM years shows a weaker and less significant change than during positive PMM years. On average, negative PMM years have 1.8 fewer TCs than the 1961–2021 climatology ($p < 0.31$) and 2.1 TCs fewer than the mean during PMM neutral years ($p = 0.24$). Moreover, the average difference of TC frequency between positive and negative PMM years is 6.8 ($p < 0.01$), implying a strong modulation of WNP TC frequency by the PMM, consistent with previous studies (Gao et al., 2018, 2020; Hong et al., 2018; Wu et al., 2020; Zhang et al., 2016, 2020). However, as noted above, the strong relationship between the PMM and TC frequency is primarily induced by the tight linkage during positive PMM years.

Figure 2 displays the spatial distributions of both the long-term climatology and the PMM-induced changes in WNP TC formation density. On average, a majority of ASON TCs form east of the Philippines (10°–20°N, 120°–150°E; Figure 2a), which is similar to the TC formation distribution during August–December (Fu et al., 2023). Compared with negative PMM years, there is an almost basinwide enhancement of TC formation during positive PMM years, except for a small region near the southern

Philippines (Figure 2b). This result is consistent with TC formation density directly regressed onto the PMM index as reported in previous publications (e.g., Fu et al., 2023; Zhang et al., 2016). In particular, over the region from 0°–25°N and 140°–155°E, TC formation density is significantly greater during positive PMM years than during negative PMM years.

The spatial structure of anomalous TC formation density during positive PMM years is similar to that of the TC formation density difference between positive and negative PMM years, with a pattern correlation coefficient of 0.76 ($p < 0.01$). The spatial structure of anomalous TC formation density during positive PMM years exhibits a more obvious basinwide enhancement of WNP TC formation than the difference between positive and negative PMM years (Figure 2c). Particularly, the anomalous TC formation density during positive PMM years significantly increases over the region of 5°–30°N and 135°–155°E, which is slightly northwestward of the significant region in Figure 2b. There are also some differences in the anomalous TC formation density pattern west of 130°E during positive PMM years between the results of Zhang et al. (2020) and ours. Zhang et al. (2020) found that there was enhanced TC formation over the northern South China Sea and suppressed TC formation near the southern Philippines, which is not shown in our results. These differences are likely caused by different PMM indices used and different seasons analysed.

By contrast, the anomalous TC formation density during negative PMM years shows no significant changes (Figure 2d). It does exhibit a different spatial pattern compared to the anomalous TC formation density during positive PMM years, with a pattern correlation coefficient of −0.06 ($p = 0.44$). During negative PMM years, TC formation is slightly enhanced west of 130°E and east of 140°E and slightly suppressed between 130°E and 140°E. The above analyses indicate that the spatial features of TC formation changes also contain an asymmetric response to the PMM.

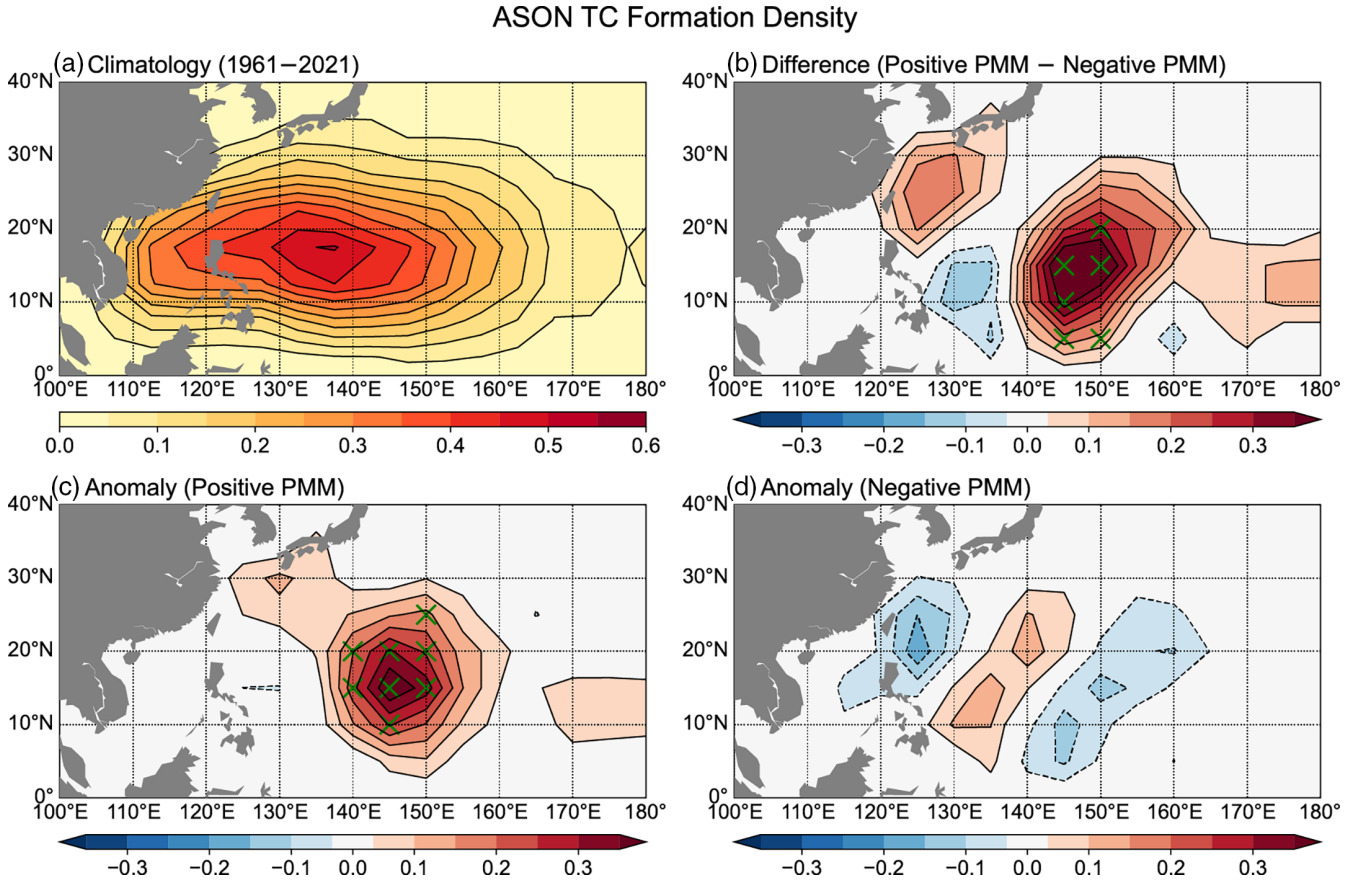

FIGURE 2 (a) Climatological average WNP TC formation density. (b) Difference in TC formation density between positive and negative PMM years. Differences significant at the 0.05 level are denoted by green crosses. (c, d) Anomalous TC formation density during (c) positive PMM years and (d) negative PMM years. Anomalies significant at the 0.05 level are denoted by green crosses [Colour figure can be viewed at wileyonlinelibrary.com]

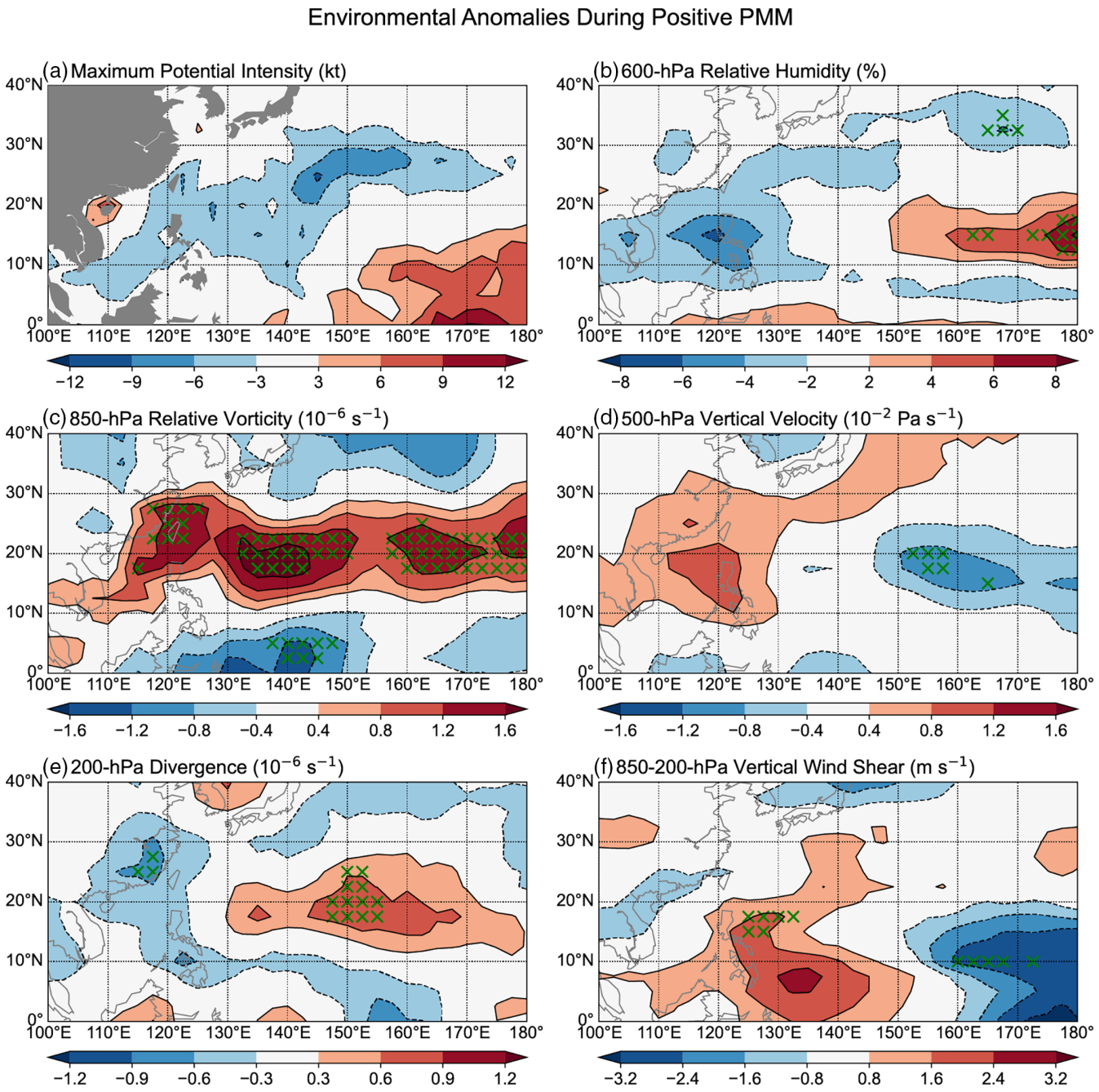

FIGURE 3 Anomalies of (a) maximum potential intensity, (b) 600-hPa relative humidity, (c) 850-hPa relative vorticity, (d) 500-hPa vertical velocity, (e) 200-hPa divergence and (f) 850–200-hPa vertical wind shear during positive PMM years. Green crosses denote anomalies significant at the 0.05 level [Colour figure can be viewed at wileyonlinelibrary.com]

4 | ASYMMETRIC RESPONSE OF ENVIRONMENTAL CONDITIONS TO THE PMM

Previous publications have shown that the modulation of WNP TC activity by the PMM can be explained by changes in large-scale environmental conditions (Fu et al., 2023; Gao et al., 2018, 2020; Hong et al., 2018; Wu et al., 2020; Zhang et al., 2016, 2020). Figure 3 displays the anomalies of environmental variables during positive PMM years relative to the 1961–2021 climatology. Compared with negative PMM years, the distributions of these environmental anomalies during positive PMM years are more consistent with those of environmental differences between the two PMM phases (figures not shown). MPI shows no significant changes over most of the WNP, while it slightly increases and decreases over the northwestern and southeastern part of the basin, respectively

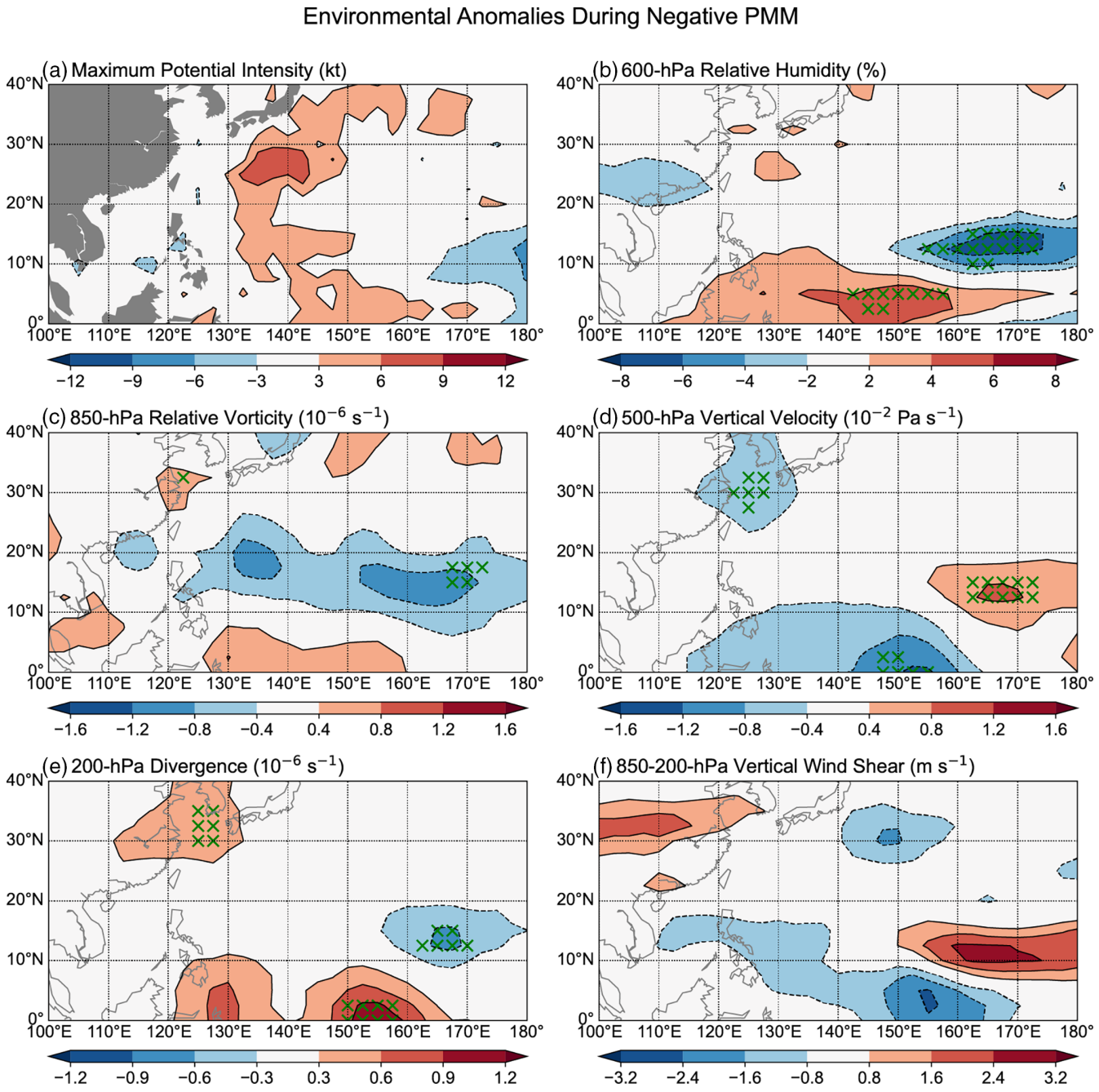

FIGURE 4 As in Figure 3, but for anomalies during negative PMM years [Colour figure can be viewed at wileyonlinelibrary.com]

(Figure 3a). Although there are significant positive 600-hPa relative humidity anomalies near the dateline, only weak relative humidity anomalies occur west of 160°E (Figure 3b). Consequently, we find that thermodynamic factors (e.g., MPI and mid-level relative humidity) play only a minor role in driving the modulation of WNP TC formation during positive PMM years.

By comparison, several dynamic factors play a more important role than the two thermodynamic factors. Over the region where TC formation is significantly enhanced (5°–30°N and 135°–155°E; Figure 2c), there are significantly positive 850-hPa relative vorticity anomalies and 200-hPa divergence anomalies as well as significantly negative 500-hPa vertical velocity anomalies (Figure 3c–e). These circulation differences imply an enhanced low-level cyclonic circulation, mid-level ascending motion and upper-level divergence, which all favour TC development. Furthermore, changes in 850-hPa relative vorticity show significantly positive anomalies within the latitudinal belt from 10°N to 30°N (Figure 3c). Given that significant vorticity anomalies correspond to a much larger part of the region with enhanced TC formation than the other two anomalies, it is

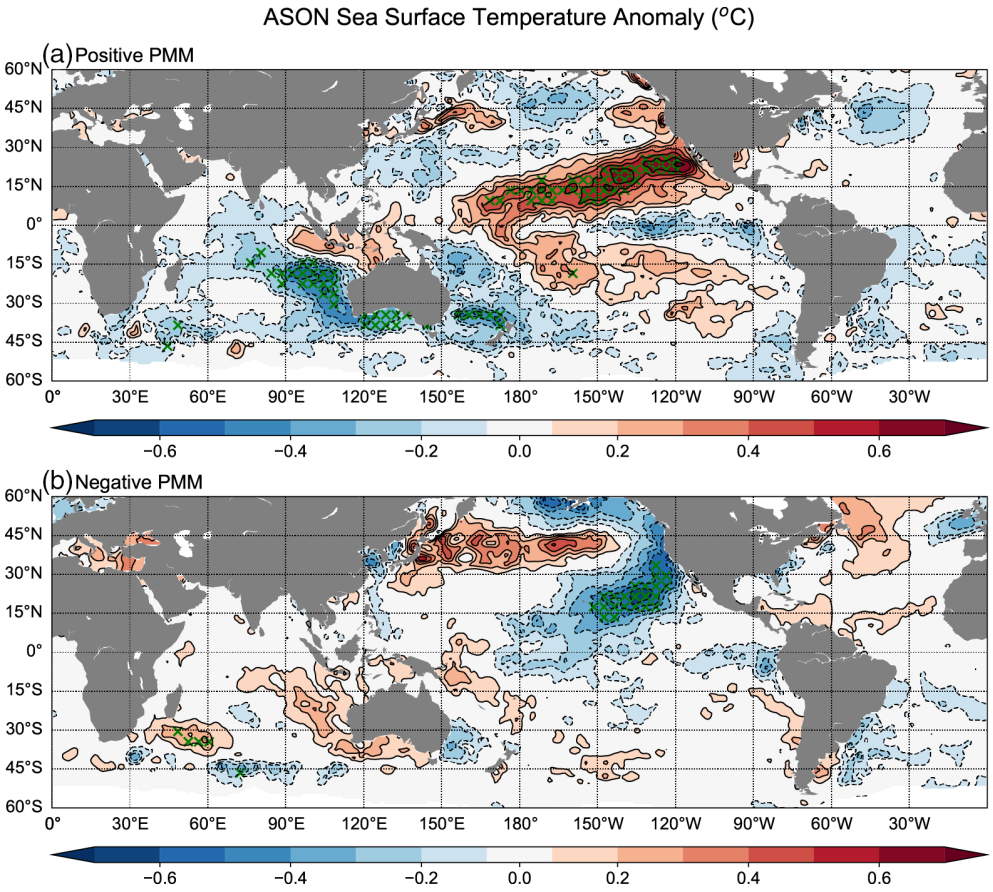

FIGURE 5 Composite SSTAs relative to the 1961–2021 climatology during ASON for (a) positive PMM years and (b) negative PMM years. Green crosses refer to anomalies significant at the 0.05 level [Colour figure can be viewed at wileyonlinelibrary.com]

likely that 850-hPa relative vorticity is the primary factor favouring WNP TC formation during positive PMM years. By contrast, although significantly increased and decreased 850–200-hPa VWSs are observed west of 135°E and east of 160°E, respectively, there are only weak VWS anomalies over the region with significant TC formation density changes (Figure 3f). These results indicate a likely lesser role played by VWS during positive PMM years.

Figure 4 displays changes in environmental variables during negative PMM years relative to the 1961–2021 climatology. In general, significant environmental changes are only found near the dateline, near the equator and near northeast Asia (Figure 4b–f), which all correspond to regions with relatively fewer TC occurrences climatologically (Figure 2a). There are almost no significant anomalies in environmental variables over the TC main development region, consistent with insignificant changes in WNP TC formation density. The spatial structure of 850-hPa relative vorticity anomalies during negative PMM years is nearly a mirror image of that during positive PMM years, with a pattern correlation coefficient of −0.54 ($p < 0.01$). However, these anomalies are of a much smaller magnitude (Figure 4c). These findings highlight that the low-level circulation patterns are symmetric between positive and negative PMM years, while the circulation anomalies during positive PMM years are much stronger than those during negative PMM years.

To further illustrate the influence of the PMM on environmental conditions, the spatial distributions of SSTA during positive and negative PMM years are first shown in Figure 5. During positive PMM years, there are significantly positive SSTAs extending from the subtropical northeastern Pacific to the tropical central Pacific, while weak negative SSTAs occur over the equatorial eastern Pacific (Figure 5a). Unlike Fu et al. (2023), we do not find a SSTA maximum over the equatorial central Pacific, due to the exclusion of positive PMMs accompanied by CP El Niños in this study. By contrast, during negative PMM years, significantly negative SSTAs are concentrated over the subtropical northeastern Pacific, while the region with negative SSTAs retreats eastward towards the dateline (Figure 5b). As expected given our PMM definition, we do not observe positive SSTAs over the equatorial eastern Pacific, while there is a latitudinal belt of large positive SSTAs in the midlatitudes of the WNP. The above results indicate an asymmetric response of Pacific SSTAs to the PMM. Fan et al. (2021) concluded that positive PMM events were generally stronger than negative ones, since they evoked stronger subtropical SST changes.

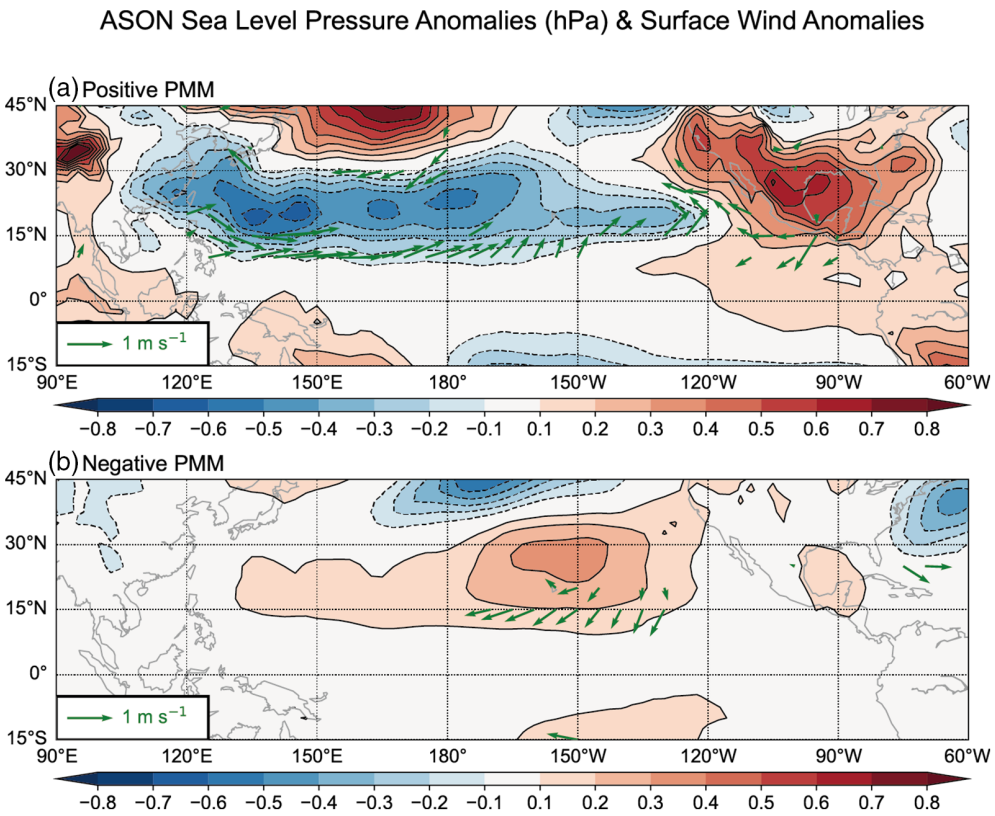

FIGURE 6 Anomalies of sea level pressure and surface wind vectors during ASON for (a) positive PMM years and (b) negative PMM years. Only wind vector anomalies significant at the 0.05 level are shown [Colour figure can be viewed at wileyonlinelibrary.com]

As reported in previous publications (e.g., Ham et al., 2013; Huo et al., 2015; Kao et al., 2022; Wang et al., 2017; Weng et al., 2022; Wu et al., 2020), trans-basin SST anomalies over the Atlantic Ocean and the Indian Ocean can influence the atmospheric circulation and TC activity over the WNP. Over the Atlantic Ocean, weak SST decreases are observed in the subpolar region during positive PMM years, while weak SST increases are observed in the tropical and subpolar regions during negative PMM years (Figure 5). There are no significant SST changes over the Atlantic Ocean, regardless of the PMM phase considered. By comparison, over the Indian Ocean, there is a weak Indian Ocean Dipole-like SST pattern during positive PMM years, while significant SST reductions are found northeast of Australia (Figure 5a). During negative PMM years, SST increases occur over most of the South Indian Ocean, with significant increases over a small region southeast of Madagascar (Figure 5b). There are no significant basinwide SST changes over the Indian Ocean during positive or negative PMM years. These results subsequently imply a lesser trans-basin influence from other basins on TC activity over the WNP, likely caused by excluding ENSO years in our PMM definition.

Subtropical SSTAs can induce atmospheric circulation changes over the Pacific via a WES feedback (Chang et al., 1997; Xie & Philander, 1994). In short, positive SSTAs over the subtropical eastern Pacific can drive an anomalous atmospheric circulation that induces a deceleration of the climatological trade winds. This further reduces the climatological evaporative heat flux over the same region, leading to a reduction in the heat loss from the ocean. This again enhances the original positive SSTAs, forming a positive feedback. Figures 6 and 7 further explain how the PMM controls changes in environmental variables through modulation of the large-scale circulation. During positive PMM years, associated with strong positive subtropical SSTAs, there are significant anomalous surface westerlies across the subtropical northern Pacific (Figure 6a). Meanwhile, a broad anomalous surface low is observed between 15°N and 30°N, with the lowest pressure anomalies occurring over the WNP. By comparison, during negative PMM years, there are significant anomalous surface northeasterlies only over the subtropical northeastern Pacific, associated with weak subtropical SSTAs (Figure 6b). The centre of the anomalous surface high shifts eastward to the eastern North Pacific, while significant surface wind anomalies are absent over the WNP. In summary, positive (negative) PMMs are characterized by a strong (weak) WES feedback. Fan et al. (2021) attributed this feature to a larger transient growth rate of latent heat fluxes during positive PMMs than during negative PMMs.

Figure 7 displays changes in PMM-induced 850-hPa geopotential height and circulation anomalies, which are similar to those at the surface. During positive PMM years, an anomalous low-level cyclone is centred over the

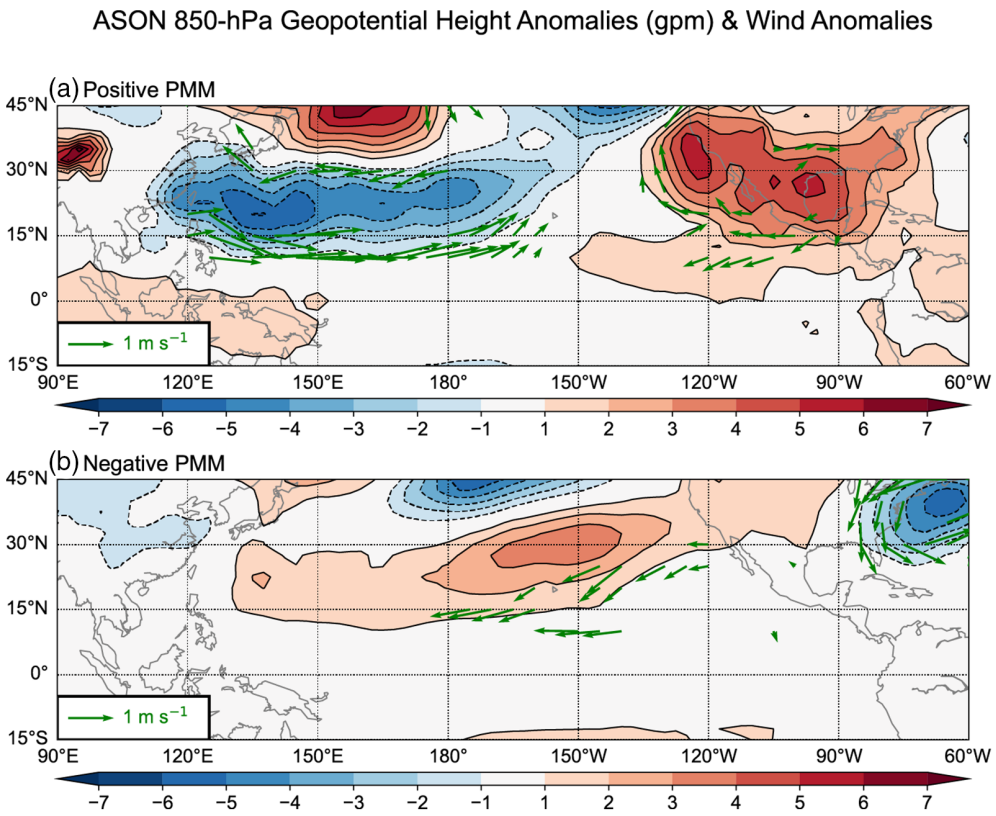

FIGURE 7 Anomalies of 850-hPa geopotential height and 850-hPa wind vectors during ASON for (a) positive PMM years and (b) negative PMM years. Only wind vector anomalies significant at the 0.05 level are shown [Colour figure can be viewed at wileyonlinelibrary.com]

subtropical WNP, with significant anomalous low-level westerlies (easterlies) along its northern (southern) edge (Figure 7a). This pattern subsequently provides significant positive vorticity anomalies that favour TC formation over the WNP. In comparison to positive PMM years, the influence of the PMM during negative PMM years is more localized over the eastern North Pacific and is not significant over the WNP (Figure 7b). An anomalous low-level anticyclone associated with anomalous low-level easterlies is observed east of the dateline. Over the WNP, there are only weak positive geopotential height anomalies, corresponding to weak and insignificant negative vorticity anomalies.

5 | CONCLUSIONS

This study investigates the asymmetric response of WNP TC formation during ASON to positive and negative phases of the PMM from 1961 to 2021. The significant correlation between basinwide TC frequency and the PMM index is predominantly induced by significantly increased TC frequency during positive PMM years, while TC frequency only slightly decreases during negative PMM years. A quadratic PMM–TC frequency relationship is more appropriate than the linear one proposed by previous publications (e.g., Fu et al., 2023; Wu et al., 2020; Zhang et al., 2016). Consistently, during positive PMM years, there is an almost basinwide enhancement of TC formation over the WNP, especially over the subdomain of 5°–30°N and 135°–155°E. This enhancement in positive PMM phases dominates the spatial pattern of the difference in TC formation density between positive and negative PMM years, given that only weak and insignificant changes in TC formation are observed during negative PMM years.

The asymmetric responses of TC formation to the PMM are further explained by distinct changes in environmental conditions over the WNP between different PMM years. During positive PMM years, there is significantly enhanced low-level vorticity, mid-level updrafts and upper-level divergence over the region of 5°–30°N and 135°–155°E, all favouring TC development. Among environmental factors, 850-hPa relative vorticity is likely to play the most important role in influencing TC formation, while thermodynamic variables (MPI and 600-hPa relative humidity) and VWS appear to have only a minor impact. By contrast, during negative PMM years, all of the environmental anomalies exhibit a smaller magnitude and are not significant over the TC main development region.

The above environmental changes of different magnitudes can be linked to differences in PMM strength. Generally speaking, positive PMM events are stronger and associated with a stronger WES feedback than negative ones. On average, a positive PMM is characterized by

significantly positive SSTAs extending from the subtropical northeastern Pacific to the tropical central Pacific, associated with anomalous surface westerlies and low-level westerlies across the subtropical northern Pacific. This subsequently provides positive vorticity anomalies over almost the entire WNP, enhancing TC formation. By contrast, the influence of a negative PMM is limited to largely the subtropical northeastern Pacific, with significantly negative SSTAs and anomalous easterlies occurring there. Hence there are almost no significant changes in large-scale circulations over the WNP induced by a negative PMM.

Our study highlights the nonlinear relationship between the PMM and WNP TC activity. Also given the asymmetric modulation of the PMM on ENSO evolution (Fan et al., 2021), other weather systems and climate modes are likely to show asymmetric responses to the PMM. One caveat of our study is that our results are obtained from a statistical analysis of a limited number of samples. These main findings will be verified by numerical sensitivity experiments considering different PMM strengths.

AUTHOR CONTRIBUTIONS

Jinjie Song: Conceptualization; investigation; writing – original draft; visualization. **Philip J. Klotzbach:** Writing – review and editing; investigation. **Yi-Fan Wang:** Validation; visualization. **Yihong Duan:** Supervision; funding acquisition.

ACKNOWLEDGEMENTS

This work was jointly funded by the National Natural Science Foundation of China (42192554, 61827901, 42175007, 41905001 and 42192552). Klotzbach would like to acknowledge financial support from the G. Unger Vetlesen Foundation.

DATA AVAILABILITY STATEMENT

All data used in this study are freely available online. Western North Pacific TC best track data provided in IBTrACS are available at: https://doi.org/10.25921/82ty-9e16. Monthly mean SST data provided by the Hadley Centre Sea Ice and Sea Surface Temperature (HadISST) are obtained from: https://www.metoffice.gov.uk/hadobs/hadisst/data/download.html. The fifth generation European Centre for Medium-Range Weather Forecasts atmospheric reanalysis of the global climate (ERA5) is retrieved from: https://cds.climate.copernicus.eu/cdsapp#!/dataset/reanalysis-era5-pressure-levels-monthly-means?tab=form. The Pacific meridional mode (PMM), Niño3 and Niño4 indices provided the Physical Sciences Laboratory of the National Oceanic and Atmospheric Administration are downloaded from: https://psl.noaa.gov/data/timeseries/monthly/PMM/, https://psl.noaa.gov/gcos_wgsp/Timeseries/Nino3/ and https://psl.noaa.gov/gcos_wgsp/Timeseries/Nino4/, respectively.

ORCID

Jinjie Song https://orcid.org/0000-0003-3948-8894

REFERENCES

Basconcillo, J., Cha, E.-J. & Moon, I.-J. (2021) Characterizing the highest tropical cyclone frequency in the Western North Pacific since 1984. *Scientific Reports*, 11, 14350.

Chang, P., Ji, L. & Li, H. (1997) A decadal climate variation in the tropical Atlantic Ocean from thermodynamic air–sea interactions. *Nature*, 385, 516–518.

Chiang, J.C.H. & Vimont, D.J. (2004) Analogous Pacific and Atlantic meridional modes of tropical atmosphere-ocean variability. *Journal of Climate*, 17, 4143–4158.

Daloz, A.S. & Camargo, S.J. (2018) Is the poleward migration of tropical cyclone maximum intensity associated with a poleward migration of tropical cyclone genesis? *Climate Dynamics*, 50, 705–715.

Emanuel, K. (2018) 100 years of progress in tropical cyclone research. *Meteorological Monograph*, 59, 15.1–15.68.

Fan, H., Huang, B., Yang, S. & Dong, W. (2021) Influence of the Pacific meridional mode on ENSO evolution and predictability: asymmetric modulation and ocean preconditioning. *Journal of Climate*, 34, 1881–1901.

Fu, M., Wang, C., Wu, L. & Zhao, H. (2023) Season-dependent modulation of Pacific meridional mode on tropical cyclone genesis over the western North Pacific. *Journal of Geophysical Research: Atmospheres*, 128, e2022JD037575.

Gao, S., Zhu, L., Zhang, W. & Chen, Z. (2018) Strong modulation of the Pacific meridional mode on the occurrence of intense tropical cyclones over the western North Pacific. *Journal of Climate*, 31, 7739–4479.

Gao, S., Zhu, L., Zhang, W. & Shen, X. (2020) Impact of the Pacific meridional mode on landfalling tropical cyclone frequency in China. *Quarterly Journal of the Royal Meteorological Society*, 146, 2410–2420.

Ham, Y.G., Kug, J.S., Park, J.Y. & Jin, F.F. (2013) Sea surface temperature in the north tropical Atlantic as a trigger for El Niño/-Southern Oscillation events. *Nature Geoscience*, 6, 112–116.

Hersbach, H., Bell, B., Berrisford, P., Hirahara, S., Horányi, A., Muñoz-Sabater, J. et al. (2020) The ERA5 global reanalysis. *Quarterly Journal of the Royal Meteorological Society*, 146, 1999–2049.

Hong, C.-C., Lee, M.-Y., Hsu, H.-H. & Tseng, W.-L. (2018) Distinct influences of the ENSO-like and PMM-like SST anomaly on the mean TC genesis location in the western North Pacific: the 2015 summer as an extreme example. *Journal of Climate*, 31, 3049–3059.

Huo, L., Guo, P., Hameed, S.N. & Jin, D. (2015) The role of tropical Atlantic SST anomalies in modulating western North Pacific tropical cyclone genesis. *Geophysical Research Letters*, 42, 2378–2384.

Kao, P.K., Hong, C.C., Huang, A.Y. & Chang, C.C. (2022) Intensification of interannual cross-basin interaction between the North Atlantic tripole and Pacific meridional mode since the 1990s. *Journal of Climate*, 35, 5967–5979.

Kim, H.-M., Webster, P.J. & Curry, J.A. (2011) Modulation of North Pacific tropical cyclone activity by three phases of ENSO. *Journal of Climate*, 24, 1839–1849.

Klotzbach, P.J. & Landsea, C.W. (2015) Extremely intense hurricanes: revisiting Webster et al. (2005) after 10 years. *Journal of Climate*, 28, 7621–7629.

Knapp, K.R., Kruk, M.C., Levinson, D.H., Diamond, H.J. & Neumann, C.J. (2010) The international best track archive for climate stewardship (IBTrACS). *Bulletin of the American Meteorological Society*, 91, 363–376.

Lee, T.-C., Knutson, T.R., Kamahori, H. & Ying, M. (2012) Impacts of climate change on tropical cyclones in the western North Pacific basin. Part I: past observations. *Tropical Cyclone Research and Review*, 1, 213–230.

Li, C., Wang, C. & Zhao, T. (2018) Influence of two types of ENSO events on tropical cyclones in the western North Pacific during the subsequent year: asymmetric response. *Climate Dynamics*, 51, 2637–2655.

Li, S., Xiao, Z. & Zhao, Y. (2023) Modulation of the influence of ENSO on northward-moving tropical cyclones in the western North Pacific by the North Atlantic tripole SST anomaly pattern. *Journal of Climate*, 36, 405–420.

Liu, C., Zhang, W., Stuecker, M.F. & Jin, F.-F. (2019) Pacific Meridional Mode-western North Pacific tropical cyclone linkage explained by tropical Pacific quasi-decadal variability. *Geophysical Research Letters*, 46, 13346–13354.

Rayner, N.A., Parker, D.E., Horton, E.B., Folland, C.K., Alexander, L.V., Rowell, D.P. et al. (2003) Global analyses of sea surface temperature, sea ice, and night marine air temperature since the late nineteenth century. *Journal of Geophysical Research: Atmospheres*, 108, 4407.

Song, J. & Klotzbach, P.J. (2018) What has controlled the poleward migration of annual averaged location of tropical cyclone lifetime maximum intensity over the western North Pacific since 1961? *Geophysical Research Letters*, 45, 1148–1156.

Song, J. & Klotzbach, P.J. (2019) Relationship between the Pacific-North American pattern and the frequency of tropical cyclones over the western North Pacific. *Geophysical Research Letters*, 46, 6118–6127.

Stuecker, M.F. (2018) Revisiting the Pacific meridional mode. *Scientific Reports*, 8, 3216.

Takaya, Y. (2019) Positive phase of Pacific meridional mode enhanced western North Pacific tropical cyclone activity in summer 2018. *SOLA*, 15A, 55–59.

Thomas, E.E. & Vimont, D.J. (2016) Modeling the mechanisms of linear and nonlinear ENSO responses to the Pacific meridional mode. *Journal of Climate*, 29, 8745–8761.

Trenberth, K.E. (1984) Some effects of finite sample size and persistence on meteorological statistics. Part I: autocorrelations. *Monthly Weather Review*, 112, 2359–2368.

Walsh, K.J.E., McBride, J.L., Klotzbach, P.J., Balachandran, S., Camargo, S.J., Holland, G. et al. (2016) Tropical cyclones and climate change. *Wiley Interdisciplinary Reviews: Climate Change*, 7, 65–89.

Wang, L., Yu, J.Y. & Paek, H. (2017) Enhanced biennial variability in the Pacific due to Atlantic capacitor effect. *Nature Communications*, 8, 1–7.

Weng, J., Wang, L., Luo, J., Chen, B., Peng, X. & Gan, Q. (2022) A contrast of the monsoon–tropical cyclone relationship between the western and eastern North Pacific. *Atmosphere*, 13, 1–22.

Wu, Q., Zhao, J., Zhan, R. & Gao, J. (2020) Revisiting the interannual impact of the Pacific meridional mode on tropical cyclone genesis frequency in the Western North Pacific. *Climate Dynamics*, 56, 1003–1015.

Xie, S. & Philander, S.G.H. (1994) A coupled ocean–atmosphere model of relevance to the ITCZ in the eastern Pacific. *Tellus A*, 46, 340–350.

Yokoi, S., Takayabu, Y.N. & Murakami, H. (2013) Attribution of projected future changes in tropical cyclone passage frequency over the western North Pacific. *Journal of Climate*, 26, 4096–4111.

Zhan, R., Wang, Y. & Lei, X. (2011) Contributions of ENSO and east Indian ocean SSTA to the interannual variability of northwest pacific tropical cyclone frequency. *Journal of Climate*, 24, 509–521.

Zhan, R., Wang, Y. & Liu, Q. (2017) Salient differences in tropical cyclone activity over the western North Pacific between 1998 and 2016. *Journal of Climate*, 30, 9979–9997.

Zhang, H., Wu, L., Huang, R., Chen, J.-M. & Feng, T. (2020) Does the Pacific meridional mode dominantly affect tropical cyclogenesis in the western North Pacific? *Climate Dynamics*, 55, 3469–3483.

Zhang, W., Vecchi, G.A., Murakami, H., Villarini, G. & Jia, L. (2016) The Pacific meridional mode and the occurrence of tropical cyclones in the western North Pacific. *Journal of Climate*, 29, 381–398.

How to cite this article: Song, J., Klotzbach, P. J., Wang, Y.-F., & Duan, Y. (2023). Asymmetric influence of the Pacific meridional mode on tropical cyclone formation over the western North Pacific. *International Journal of Climatology*, *43*(14), 6578–6589. https://doi.org/10.1002/joc.8220